Chemical Engineering Journal 158 (2010) 69–77

Contents lists available at ScienceDirect

Chemical Engineering Journal

journal homepage: www.elsevier.com/locate/cej

Electrical resistance tomography for characterisation of physical stability in liquid compositions

Adam Kowalski[a], John Davidson[b], Mark Flanagan[a], Trevor York[b,*]

[a] Unilever R&D Port Sunlight Laboratory, Quarry Road East, Bebington, Wirral CH63 3JW, UK
[b] University of Manchester, School of Electrical & Electronic Engineering, UK

ARTICLE INFO

Article history:
Received 22 April 2008
Received in revised form 19 October 2009
Accepted 23 October 2009

Keywords:
Electrical resistance tomography
Product ageing
3D image reconstruction

ABSTRACT

The paper describes experiments to investigate the feasibility of using electrical tomography for early characterisation of physical stability in selected products. The Manchester LCT tomograph has been applied to an 8-plane sensor hosted in a 1-l vessel. Measurements have been taken over periods up to 76 h. Tomographic measurements and reconstructed images are consistent with visual observations associated with experiments that readily generate a distinct visible 'separated layer'. Observed diurnal excursions in the measured voltages have been investigated and related to changes in temperature. Later experiments have been performed in a temperature controlled environment. Conductivity changes have been extracted from the reconstructed images for selected pixels. These reveal behaviour which is indicative of instability prior to visually discernible effects.

1. Introduction

The paper describes work to explore the feasibility of using electrical resistance tomography (ERT) for characterisation of physical stability in multiphase liquid compositions. Fluid preparations which consist of multiple, non-miscible ingredients have a tendency to change over time and can suffer from both physical (e.g. creaming) and colloidal (e.g. coalescence) stability problems [1]. Such preparations are common in many formulated products sold to the public including cosmetics, paints, pharmaceuticals, detergents and processed foods. Similarly in business to business transactions raw material suppliers are increasingly providing their customers with preparations (i.e. suspensions and emulsions) which are easy to handle, incorporate and disperse. For all of these applications the formulated products must remain physically and colloidally stable over timescales ranging from minutes to hours, days, weeks, months and, in the case of some of the products mentioned above, for several years [2].

Typically, during product development, manufacturers must conduct extensive storage trials over representative timescales in order to assess the impact of formulation and process changes. Such testing is time consuming and labour intensive and often such measurements are not technically demanding (e.g. height of sediment). Consequently there is a real need for techniques which are capable of either measuring creaming or sedimentation accurately and automatically or are able to detect changes which signal the onset of instability. The value of such techniques is in the freeing up of valuable resources (especially research staff) to concentrate on developing scientific insights which can generate real performance improvements in products or speed up the innovation process. A wide range of measurement techniques have been considered which can be broadly characterised as accelerated testing, point measurement and tomography. Accelerated testing [1] has historically been predominantly used in industry although modern measurement capabilities offer the intriguing possibility of a "high throughput" and/or characterisation of early stage features which are indicative of long term stability. Accelerated testing relies on modifying some external influence, for example gravitational force, through centrifugation or temperature to reduce viscosity and accelerate colloidal processes. However in practice these techniques can be severely limited in that other physical or colloidal changes may alter stability and give misleading results. For example, the emulsifying power of a non-ionic surfactant is temperature dependent and performance deteriorates or improves with temperature [3,4]. A variety of point or local measurement techniques have also been considered including laser light scattering [5], vibrating reeds [6] and ultrasonics [7]. In many cases the interface (sometimes called the mud line) in a sedimenting system is diffuse and not easily determined [8]. Point measurement techniques can be positioned at various positions (e.g. [6]) but are only sensitive to local changes whereas tomography offers full 3D monitoring.

* Corresponding author at: School of Electrical & Electronic Engineering, University of Manchester, Sackville Street, PO Box 88, Manchester M60 1QD, UK.
Tel.: +44 0161 306 4729; fax: +44 0161 306 4789.
E-mail address: t.a.york@manchester.ac.uk (T. York).

1385-8947/$ – see front matter © 2009 Elsevier B.V. All rights reserved.
doi:10.1016/j.cej.2009.10.054

Sedimentation or creaming is a commonly observed phenomenon in both industrial and natural situations and ERT has proved a useful tool in its study. Separation can be both desired such as in separation processes [9,10] or avoided such as waxes in crude oil [11], paints and adhesives [12], particulates during pharmaceutical processes [13], sedimentary basins [14] and cosmetics and personal care products [1,2,15].

Formulated products of the type considered here form the basis of many consumer products in the food and personal care areas. An example includes surfactant phases—either worm-like micelles or dispersed lamellae—which are extremely useful in commercial products because they are very weight-effective at building viscosity [16,17]. The challenge is to identify the features of the microstructure which give rise to differences in stability as well as rheology and use this understanding to manufacture products with improved performance [18]. A particular example of a surfactant based liquid crystal system which has a number of interesting features is the lamellar phase and in particular the dispersed lamellar system. Lamellar phases can be formed from a wide range of materials, including non-ionic, anionic and cationic surfactants and block copolymers [19]. Lamellar systems, in common with other surfactant phases such as worm like micelles, are effective at building bulk viscosity at low concentrations (<5%).

The products used in this study are commercially available and comprise a mixture of water and surfactants. The surfactants are quaternary surfactants and a fatty alcohol co-surfactant and the product consists of a dispersed lamellar phase [20,21]. The formation of the dispersion is sometimes referred to an emulsification with an effective surface tension which can be used to predict drop size in response to a deformation [22]. Whilst this analogy has its uses we should recognize one important difference—true emulsions have a distinct interface between the oil and water phases whereas in the dispersed lamellar phase there is no such interface and individual components (e.g. water or salts) can reside in both the dispersed phase and the continuous phase. What is more probable is that there is a concentration gradient of ingredients between the dispersed phase and the continuous phase. This is also strongly supported by the observation that dispersed lamellar phases tend to be opaque whilst the continuous lamellar phase tends to be translucent or even clear. One interesting consequence of these considerations is the composition of both the dispersed and continuous phase can vary even between products of the same formulation thus making the idea of a calibration meaningless. Szymanski et al. [21] have shown recently that the continuous phase viscosity of such a system is about twice that of water for samples with differing rheological profiles and furthermore that the system contains freely diffusing vesicles of about 100 nm. Moreover the rheology of such a composition can be modified by a wide range of variables such as the composition [19,20,23–25], deformation [26,27], order of addition [28] and temperature [29]. Nevertheless this complex behaviour coupled to the practical consideration of differences arising from inter-batch variability of raw materials presents a clear challenge to any measurement technique that characterisation should not depend on calibration.

Section 2 describes the hardware and software that has been used to explore the potential for electrical tomography in characterising the physical stability of liquid compositions. Section 3 describes the experiments that have been performed and Section 4 presents results.

2. Hardware and software

2.1. Tomograph

The Manchester LCT instrument [30] has been used to acquire the tomographic measurements. This instrument was originally designed to provide low-cost access to electrical tomography for feasibility studies and research. The LCT system employs digital signal processing algorithms to obtain the amplitude and phase of signals from rapid sampling of voltages on a signal conditioning board. The system can provide sinusoidal signals from a few Hz up to 1 MHz from an ADS7008 DDS chip. Differential current is provided on two terminals and the value is determined from the potential drop across a sense resistor. Differential voltage is measured on two other terminals and converted using a 16-bit ADC. The four terminals on the signal conditioning board can be selectively connected to any electrode using a cross-bar switch that can host up to 64 electrodes. The settling time of the present switching components limits the data rate to about 300 measurements/s. For a "conventional" 16 electrode system this equates to a modest acquisition rate of about 1 frame/s. The LCT is interfaced to a host PC via a USB2 link that can operate up to about 20 MBytes/s. The instrument is housed in a small unit measuring 22 cm high × 18 cm wide × 27 cm deep.

The LCT is designed for versatility and accessibility of data to facilitate exploratory research. A valuable feature is that electrode excitation strategies are not restricted to conventional approaches such as the "adjacent" method and therefore process compliance can be accommodated. Bespoke software has been written to control the LCT hardware and acquire measurements. For the present work the tomographic measurements are exported as an ASCII text file which is then imported into Matlab for further processing to yield 3D tomographic images.

2.2. Sensor

The characterisation of physical stability is important both during manufacturing processes and, as described here, during long term storage tests. At manufacturing scale physical stability is particularly important in intermediate storage vessels (diameter >1 m) where there is often no externally driven mixer to main homogeneity. Typically timescales here are of the order of minutes to hours and the aim is to ensure that the product feeding the filling lines is homogeneous in each and every bottle which may number as many as many as 20,000 bottles. However in this study we are much more interested in the long term stability at the scale of the bottle. Most electrical tomography applications have involved dimensions from about 5 to 30 cm. Some work has been reported on a production pressure filter of 4 m diameter [31,32]. Therefore, it is feasible to consider scale up or down as far as the technique is concerned. Clearly the larger the vessel then the smaller the overall wall effect. However, for larger vessels it is also necessary to employ larger excitation currents in order to generate measurable voltages.

In order to pursue applications such as this it is not always straightforward to have access to readily-assembled sensor vessels. For this work a vessel has been designed based on a 1-l "tall-form" beaker as shown in Fig. 1. The sensor electrodes are fabricated as flexible printed circuit boards that are attached as vertical strips on the inside of the beaker. The electrodes are gold plated and connections are taken out to the LCT using a 20-way FFC socket. Extensive modelling of the vessel was undertaken by FEM to facilitate subsequent image reconstruction. Vessel modelling suggested that the accuracy of sensor placement need only be within a few percent of the vessel diameter. Fig. 2 shows an example of separation, indicative of product instability, during the experiments.

Vessel construction uses a combination of non-corrosive silicone sealant and pressure sensitive adhesive tape to mount the flexi-PCBs firmly on the glass wall. Generally, the vessels performed well and in the event of a sensor failure it was a straightforward task to replace a single flex-PCB strip. However, after about two weeks of experiments it was clearly evident that the surface of several of

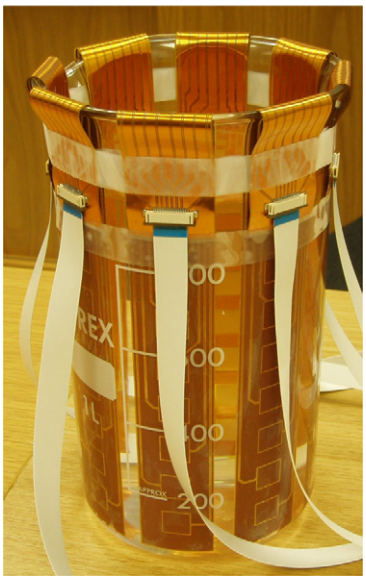

Fig. 1. Sensor vessel.

the electrodes had deteriorated noticeably; the gold surface was no longer present and a dark blackish colour existed over large proportions of the affected sensor. This was found to be the case in about 10% of the electrodes and is believed to be due to oxidation of copper that is exposed by detachment of the gold plating. The significance on the measurements due to this phenomenon is not known, however it was deemed good practice to replace any degraded electrode strips. In future this could be avoided with improved fabrication and materials.

2.3. Image reconstruction algorithm

The EIDORS-3D tool-suite [33] has been used to solve both the forward and inverse problems in the Matlab environment with a standard desktop PC. The process of image reconstruction requires a solution to be found which relates each part of the image space to the measurement data by solving a set of simultaneous equations. In the present case, the problem has been discretized into a 3D Finite Element Model (FEM) of the vessel comprising 3385 tetrahedral elements describing the interior space and 64 electrodes as shown in Fig. 3.

Fig. 2. Example separation.

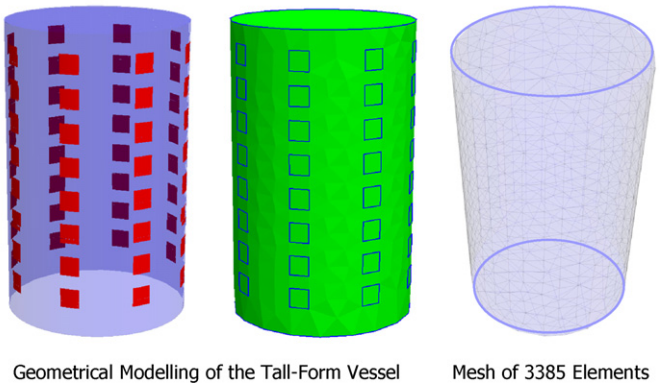

Fig. 3. Discretisation of the sensor vessel.

As is widespread in Electrical Impedance Tomography (EIT), this study assumes a linear approximation of the soft field problem and attempts to calculate the unique conductivity distribution, σ for a set of voltage measurements, V_m normalised to the actual injected electrode currents. This can be described as:

$$\sigma = J^{-1} V_m \tag{1}$$

where "J" is the Jacobian matrix which relates a small change in the conductivity distribution to the corresponding changes in the measurement vector and is calculated throughout the whole of the image space for the complete measurement vector. However, a direct solution to Eq. (1) does not exist due to the highly ill-conditioned nature of "J" and the inability to perform a direct matrix inversion. To overcome this problem, this study used a generalized Tikhonov regularization method. The regularization has the advantage of improving the reliability of the inverse solution. The method can be described by the following equation:

$$\sigma = (J^T J + \alpha I)^{-1} [J^T (V_m - V_{fr})] \tag{2}$$

where "I" is a unity matrix, "α" is a regularization parameter and "V_{fr}" is the predicted voltage vector on the electrodes from the forward solution. The above method has been shown to give reconstruction of good spatial fidelity and has been described in more detail by Davidson et al. [32]. Additionally, a mathematically similar method to the above has been compared with other reconstruction techniques elsewhere [34]. This present study pre-computes "$J^T J$" for the test vessel and solves Eq. (2) in a single-shot manner without iteration. It employs a difference imaging technique relative to an absolute reference image at the start of the experiment prior to any phase separation. The reconstruction was repeated for all data frames relative to the same initial reference image. The reconstructed difference image, "σ_{diff}" for a particular frame in time can be described by:

$$\sigma_{diff} = \sigma_{t=T} - \sigma_{t=0} \tag{3}$$

where "$\sigma_{t=0}$" is the calculated reconstructed conductivity prior to phase separation and "$\sigma_{t=T}$" is the calculated reconstruction for a frame of interest. The difference imaging approach has the distinct advantage of removing any uncertainty in parameters such as contact impedance or minor inaccuracies in modelling the test vessel. Using normalised data does not significantly affect the processing time. If conductivity changes are smaller than the measurement error then the slow dynamics of the process mean that improved statistics can be exploited by acquisition over longer periods. A further consideration is the effect of changing the mesh density. This might be increased in an effort to reduce noise. However, the major

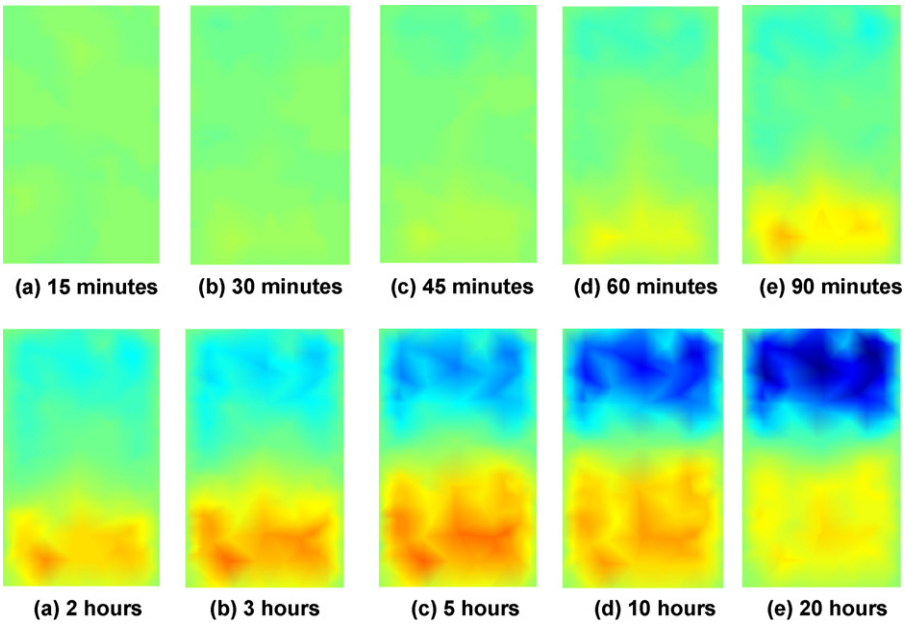

Fig. 4. Image reconstruction for batch "A" in the vertical *x*–*z* planes. Product mixed with water and salt in the proportion 20%:79.75%:0.25%.

contribution to this noise is likely to be as a consequence of the level of smoothing applied within the inverse solution, namely the regularization parameter. The choice of regularization is one of the key aspects for image reconstruction and depends on the model, sensitivity map and nature of the measurements. Too much smoothing and the reconstructed image will display very little change. Too little smoothing and the image will just display the sensitivity map. The regularization parameter is, effectively, a way of distinguishing between the high and low frequency spatial components in the image space. Additionally, if the mesh density is increased too much, the "posed-ness" of the problem could be too great to find the correct solution from the adopted inverse algorithm. For the present work control parameters for the image reconstruction algorithm were selected by intuition and experience. More recently we have explored improved methods for selection of the regularization parameter using the Discrete Picard Condition [35]. Typical time for reconstruction using a desktop PC was in the order of 20 s/frame of data.

3. Experiments

The LCT offers unfettered exploration of electrode excitation strategies. For this work an optimised measurement strategy was determined by simulation and simple "water and rod" tests in order to give the most uniform sensitivity map. The outcome is a strategy yielding a total of 1104 measurements by injecting currents on in-plane adjacent current pairs but only considering adjacent horizontal voltage measurement pairs in the injection plane and on planes *immediately* above and below the injection plane. In order to display image reconstructions as vertical slices (*x*–*z* and *y*–*z* planes) it was necessary to develop bespoke Matlab code for use with EIDORS-3D.

A number of experiments have been undertaken using two batches of material "A" and "B". To promote instability the products have been mixed with varying proportions of water and a small quantity of salt. For comparison, control tests have been carried out using unadulterated product under the same conditions in order to determine the significance of any tomographic measurement changes. Data analysis can be divided into raw data: 3D image reconstruction and extraction of temporal variations in voxel values. The two batches showed different behaviour. Specifically, sample "B" was found to give less separation when mixed with a relatively low proportion of water compared with the same experiment using sample "A". Additionally, sample "B" was much less viscous in nature. This type of variation in commercial products is to be expected since quality control parameters tend to have a range within which the end use performance is unaffected. It does however emphasise the need for measurement techniques that can predict ageing and stability without the need for calibration.

4. Results and discussion

4.1. Results of image reconstruction

For experiments involving batch "A" an initial reference frame was generated from the average of five frames acquired over a 1 min interval. Thereafter, the frame rate was set to 15 min and continued for times varying between 20 and 80 h. In all reconstructions the differing shades of red and blue refer to the levels of reconstructed conductivity with respect to the initial 'reference'. Darker shades of red suggest 'more conducting' with respect to the initial frame which is normalised to "green". Conversely, shades of blue are a measure of voxels becoming 'less conducting' with respect to the initial frame. To facilitate viewing in greyscale the reconstructions are discussed at appropriate places in the text. Representative images are shown in Fig. 4, obtained using batch "A" mixed with water and salt in the proportion 20%:79.75%:0.25%. These values were chosen following experiments to find a mixture that separated in a reproducible way over a relatively short time period. The images show that over time the upper regions become less conducting (more "blue" compared to the initial "green" state) whilst the lower regions become more conducting (more "red"). In greyscale the initial state appears as light grey. The less conducting regions, towards the top, appear as almost black whilst the more conducting regions are grey.

For experiments involving batch "B" data have been acquired every 77 s over approximately 6 h to yield improved temporal resolution. These experiments were carried out in a controlled environment which maintained the temperature to within 2° of 18 °C. Further discussion relating to the effect of temperature is included

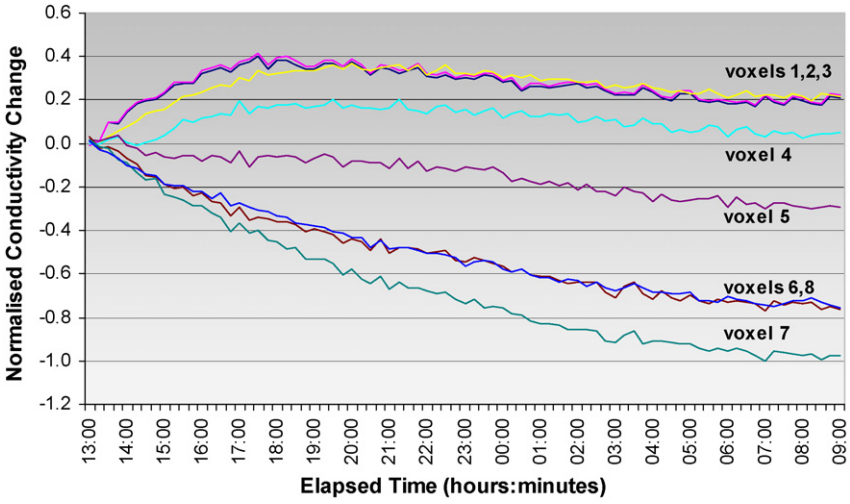

Fig. 5. Voxel extraction for product batch A corresponding to images in Fig. 4. Product mixed with water and salt in the proportion 20%:79.75%:0.25%.

in Section 4.3. The measured conductivities are determined from samples that have been 'extracted' from a test sample and show that the greatest conductivity change with respect to the initial mixture is for the upper layer, whereas the lower layer shows a relatively small change. This is consistent with the reconstructions and is a crucial validation result. As for batch "A", over time the upper regions become less conducting whilst the lower regions become more conducting.

4.2. Voxel extraction from images

Reconstructed images are highly useful for visualizing the overall nature of a system from the tomographic measurements. However, from images alone, it is not always possible to discern fine detail in the regions of interest. For this reason an alternative and potentially more useful approach is to extract sample voxels from the image space and shows graphically the behaviour of the data within such voxels. A bespoke Matlab 'tetrahedral searching' code has been used to extract a total of eight single voxels from specified locations within the mesh of the modelled vessel. These voxels are approximately equi-spaced along the vertical axis and in the centre of the vessel. Voxel "v1" is the lowest and "v8" is the highest along the axis.

Voxel extraction has been applied to data corresponding to Fig. 4 over a period approaching 24 h and the results are shown in Fig. 5. The solution data are represented as normalised conductivity changes that are referenced to the greatest observed change during data collection—in this case represented by voxel 7 towards the top of the vessel. Clear differences can be seen in the temporal evolution of the voxels, particularly changes in the gradients. This strongly suggests that electrical tomography is capable of identifying physical/chemical changes within this type of system even for regions which apparently show no visible change, notably the upper part of the vessel. It can also be seen that the voxel data broadly fall into two distinct regions: the lower voxels (v1–v4) yield solution data that become positive with respect to the starting condition whilst the upper voxels (v5–v8) yield negative changes. These observations are consistent with visual observations.

The products separate into two distinct layers, as shown in Fig. 2, with a lower level of semi-transparent liquid and an upper "white" level. These two layers correspond to voxels 1–4 and 5–8 respectively. The phase separation is a consequence of the density difference between the continuous phase, which predominantly contains water and salts, and the dispersed phase, which in addition contains the fatty alcohol and so is less dense. The profiles may be interpreted in terms of separation of high phase volume systems. In this case the separation is creaming so that at the bottom there is an isotropic fluid which is essentially the continuous phase of the dispersion. Voxels 1–3 have very similar profiles (though v3 lags v1and v2) indicating that the composition in these regions must be similar and is essentially an isotropic solution of water and salts. Voxel v4 lies just below the separating boundary and although still positive relative to the initial conditions its behaviour is clearly distinct from voxels v1–v3. The interface between the separating phase and the isotropic lower level is unlikely to be sharp and suggests that there may still be some dispersed phase in the vicinity. The phase volume in this region may be substantially lower than the maximum packing fraction and so the creaming of the individual lamellar fragments will be Stokesian with the rate lower for smaller and more neutrally buoyant particles. Moreover the electrical field generated during the measurement has a 3D character and so is sensitive to materials out of the plane of the sensor ring.

In the packed bed at the top of the sample the density gradient will drive the denser phase (i.e. the continuous phase) downwards and the concentration of lamellar fragments will be highest near the surface. Thus we see from voxels 5 to 7 a family of curves of increasingly negative value (Fig. 5) and this is consistent with an increasing concentration of lamellar fragments towards the top of the sample. The electrical properties of structured products have not been studied in as much detail as a simple solution but dielectric measurements have shown sensitivity in response to compositional changes [36], to changes in microstructure which arise from the intensity of the manufacturing process [37] and to changes in the phase behaviour of liquid crystal gels and even the location of added ingredient in the liquid crystal structure [38]. Whilst we only consider a single frequency in this study it is entirely possible, and indeed likely, that the reconstructed data reflect local compositional or microstructural variations. Of particular note is that the long time discrimination between the voxels is apparent shortly after the start of the experiment and before a clear separation of the phases is seen. This presents the intriguing possibility that we might use the very early shape of the profiles as an indicator of long term behaviour.

Finally, we should note that the conductivity trajectory displayed by voxel 8, although still negative relative to the starting condition, does not lie in sequence with the other voxels. This is likely to be a consequence of the proximity of the surface affecting the reconstruction.

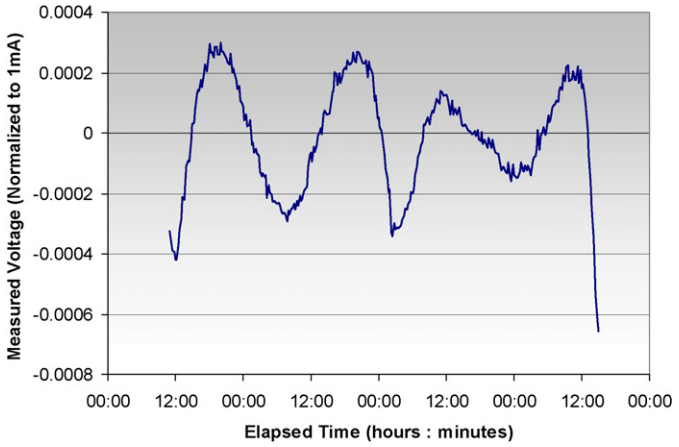

Fig. 6. Diurnal variation in voltage measurements. Current injected on electrodes "1" and "2"; voltages are measured on electrodes "5" and "6".

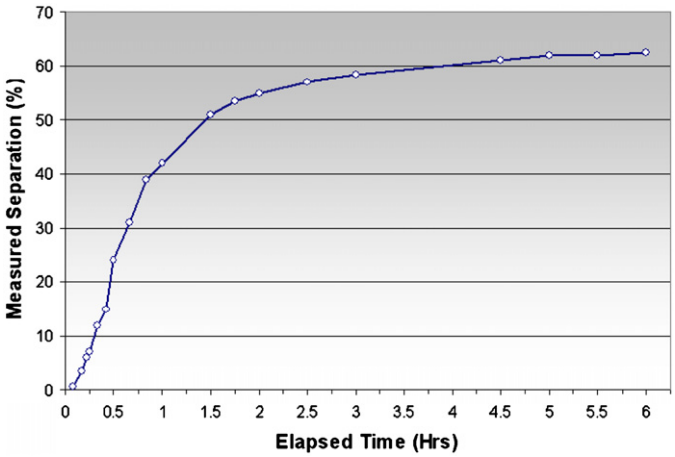

Fig. 7. Visually observed separation for batch B. Diluted in the ratio 20:79.75:0.25 of product:water:salt.

4.3. Influence of temperature changes

In performing the experiments it became apparent that changes in temperature might be influencing the measurements. In order to ascertain the magnitude of the effect measurements were observed over 3 days. Fig. 6 shows the resulting time plot for the change in measured voltage over 3 days. This corresponds to the case when current is injected on electrodes "1" and "2" and voltages are measured on electrodes "5" and "6". The periodic variations are clearly evident and these would seem to be linked to a daily period. This is perhaps not surprising as the laboratory temperature changes by a few degrees during the course of a day, being warmest in the afternoon and coldest during the night. The amplitude of these variations corresponds to about 4% of the overall measured signal strength. This should be compared with the observed changes due to ageing which are about 18%. Consequently it can be deduced that the observed measured changes due to ageing are significant compared to changes due to temperature variations. However, as a consequence, later experiments were conducted in an environment in which the diurnal temperature variation was only about 2 °C. Nevertheless stability testing with temperature cycling such as freeze–thaw [1] is commonly used and the current results indicate that although temperature has an impact on the reconstruction it is possible to separate out the changes due to temperature cycling from those due to stability problems.

It is apparent from Fig. 6 that the diurnal variation is not consistent and further study is needed to compensate for this effect. However, in practice, storage trials are conducted in climatically controlled rooms where temperature is carefully monitored for deviations. In some instances the temperature is kept constant to within a degree but in others it is cycled to expose products to conditions that mimic real life, for instance, freeze–thaw cycles. Consequently in practical situations there will be an independent measure of temperature which can be used to compensate for the tomography measurements. Perhaps more interestingly tomography could provide valuable insights into the rate at which temperature variations in the product reflect externally driven cycles. For example, the thickness and thermal properties of the pack wall, the shape and size of a product pack, the thermal properties of the product and also the position of the sample pack in the climatic store all affect the heat transfer rate. As a consequence the degree to which the material in the bottle actually sees the extremes of the temperature cycle will vary and impact the validity of such product testing.

4.4. Results with controlled temperature

Voxel extraction has been applied to batch "B" with a data collection rate of 77 s between frames, in order to determine if the tomographic measurements can expose the very early onset of any observed physical and/or chemical change. These tests were carried out in an environment where the ambient temperature was stable within 2 °C. Additionally, the physical separation occurred relatively quickly compared with batch "A". Fig. 7 shows the results of visual observation of separation over 6 h for batch "B" mixed with water and salt in the proportion 20.00%B/79.75%W/0.25%NaCl (i.e. identical to that for batch A). This is expressed as a percentage of the height of the product in the vessel. The faster separation observed in "B" for essentially the same conditions as those for "A" illustrates the industrial processing challenge. Essentially the starting products are identical and within specification and yet they exhibit different stability behaviour. How can we distinguish between these two products shortly after manufacture without the need for long term stability testing?

Extracted voxel data for the related 'control' showed little change beyond the noise level. However, for batch "B" diluted with water and with added salt the changes are most apparent from the tomographic measurements as shown in Fig. 8. Similarly to the previous voxel extraction example shown in Fig. 5 the conductivity changes are normalised and differences in gradients can be seen even for the uppermost planes. Again we see increasingly nega-

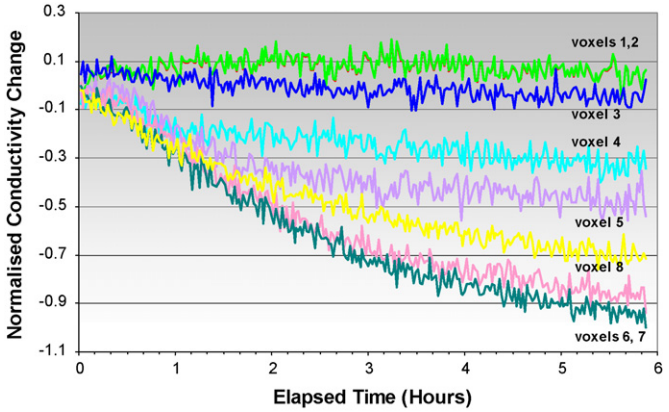

Fig. 8. Voxel extraction for product batch B which was diluted in the ratio 20:79.75:0.25 of product:water:salt. Experiment performed at constant temperature.

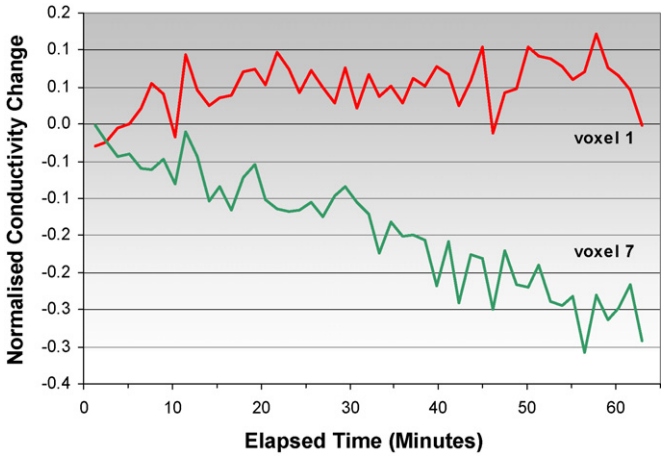

Fig. 9. Voxel extraction in the first hour of experiment shown in Fig. 8.

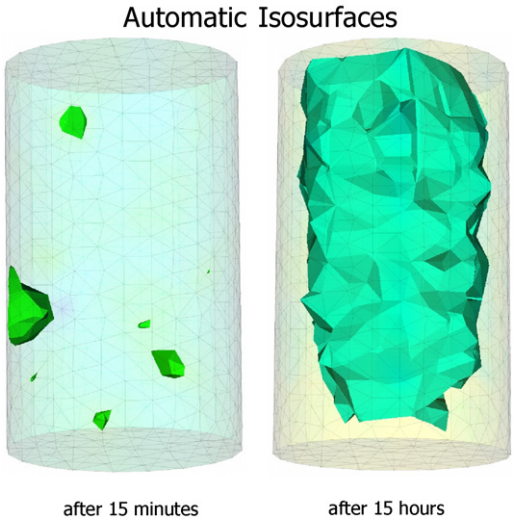

Fig. 11. Reconstructed isosurfaces.

tive values as we move from the bottom (v1) to the top (v7) of the vessel and again v8 does not follow the sequence. Fig. 9 shows an expanded view of the same data for the first hour and just two voxels, "v1" (towards the bottom of the vessel) and "v7" (towards the top of the vessel). It is immediately apparent from this data that the tomographic method has been very successful in identifying changes in the first few minutes of the experiment. This is significant as no changes were apparent during this period from visual observation alone. Additionally, and crucially, the changes are strongly apparent for not only the voxels associated with the lower half of the vessel but also those from the upper half. This experiment suggests that a potentially useful indicator of early onset of ageing (or separation) may be associated not just with data from the lower part where an isotropic layer forms but also tomographic data extracted from the upper part of the product.

4.5. Tending towards the real case

The results presented above represent "manufactured" situations in which ageing is accelerated by the addition of salt and water. Efforts were also made to explore more realistic instabilities, over a timescale of days rather than minutes or hours. In this case the visible separation barely reached the lowest plane of electrodes after 2 days. However, despite this relatively subtle change, the image reconstruction after 48 h shows a distinct interface at the bottom of the vessel which is similar in height to the observed semi-opaque layer as shown in Fig. 10. This is highly encouraging and suggests a good level of sensitivity despite the relatively 'coarse' mesh with only 3385 tetrahedra. It is anticipated that sensitivity could be improved further by inclusion of base-mounted electrodes and solving over a more finely resolved mesh. Clearly further work would be required to follow commercially viable products over several months to form a link between the early indicators of change in the product with the long term stability.

Data obtained using the unadulterated product have been viewed using MayaVi visualization software as shown in Fig. 11. The superimposed mesh shows the effective 'limit of resolution' of the reconstruction. This could be improved significantly using a finer mesh. It should be noted that the generated isosurfaces are found automatically by the MayaVi software which identifies the greatest change in the gradient across the entire solution. The value at which this occurs is used to 'link' all other data having this value. In this case, the procedure requires *no* manual intervention. The isosurface for the data after 15 h is shown in Fig. 11 and suggests the existence of a distinct separated layer (due to conductivity changes) which could not be discerned by visual inspection.

Fig. 12 reproduces the single voxel extraction from the data set and is to be compared with Figs. 5 and 8. It should be noted that for Fig. 12 all voxels show a negative change in their value over time whereas in the previous samples we saw positive changes. However we also note that once again voxels v1–v7 form a family

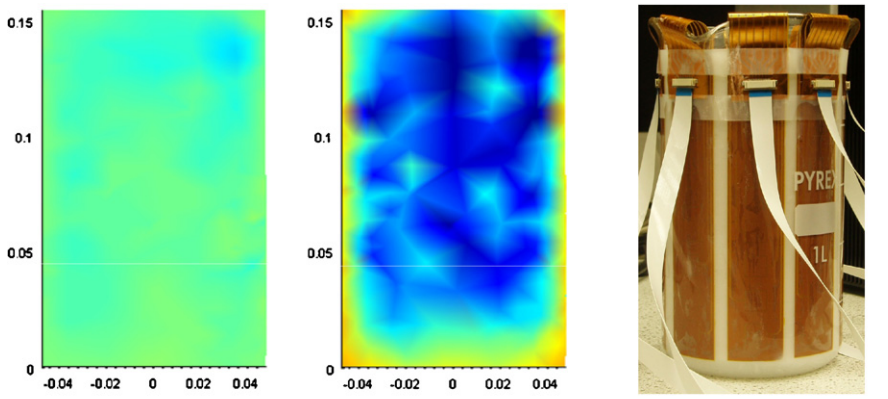

Fig. 10. Image reconstruction for unadulterated product. The central dark (blue) region corresponds to regions of relatively low conductivity. (For interpretation of the references to colour in this figure legend, the reader is referred to the web version of this article.)

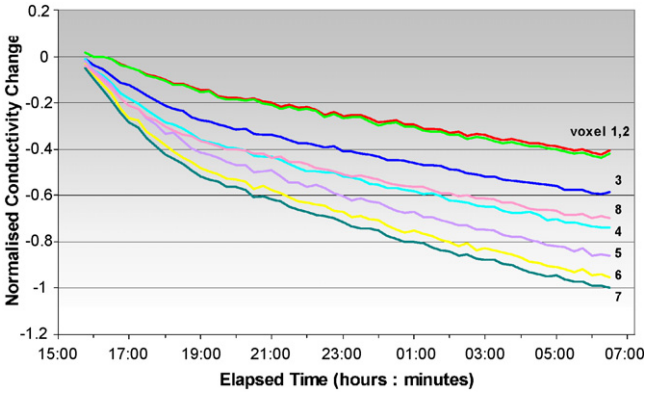

Fig. 12. Single voxel extraction from the solution data for the unadulterated product.

of curves with increasingly negative values from the bottom of the sample (v1) to the top of the sample (v7). In particular v1 and v2 are very similar which are again consistent with seeing an isotropic layer forming at the bottom as the dispersed phase creams. Finally the topmost voxel (v8) does not follow the sequence as observed in the earlier example.

The family of curves obtained from voxels v1–v7 indicate that, even for this unadulterated sample, bottom to top changes can be picked up by ERT and that these changes are observed in advance of visually observable changes. The fact that we do not observe positive changes in the voxels closer to the base of the sample can perhaps in part be attributed to the absence/presence of salt. In the earlier example the presence of the added salt will dominate the conductivity of the isotropic phase so that as the lower conductive dispersed phase creams the conductivity will increase. It is however less clear to the mechanisms in the unadulterated case with no added salt. The data suggest that the sample as a whole decreases in conductivity although no measurements were made with conventional conductivity probes. Some insight can be generated by comparison to the rheology of liquid crystal systems which changes in time and has a thixotropic nature [21]. Such rheological changes arise from changes of the microstructure (e.g. the size, shape and degree of flocculation) and it may reasonably be expected that such changes might also give rise to changes in conductivity. Next we note that microstructure is sensitive to deformation as might, for example, result from pouring the sample into the ERT vessel. In rheological measurement, for example, it is usual to allow the sample to "rest" prior to commencement of the measurement. Thus we might hypothesise that the wholly negative trends in the voxel extractions reflect firstly top to bottom separation and secondly the relaxation of the structure following the disturbance of transferring the sample to the ERT vessel. It should be noted that the images in Figs. 4 and 10 suggest some radial dependence on the conductivity distribution, notably a possible wall effect. This should be explored in further work.

5. Summary

A feasibility study has been undertaken to explore the use of electrical resistance tomography for detecting early onset of ageing in formulated products. Experiments have been undertaken using a "tall-form", 1-l, beaker which has flexible electrode strips attached on the inside wall. This "sensor" vessel has been specially designed to facilitate ready exploration. A "product" has been deliberately adulterated using salt such that the ageing process is accelerated. The feasibility study has produced highly encouraging results. The reconstruction algorithm coupled to extraction of trends for voxels at various heights of the vessel have shown features which are consistent with the observed separation behaviour. Encouragingly the early onset of separation seems to have been picked up not just with sensors close to the separation region but also by those in other locations.

The influence of temperature variation on the instrumentation is amplified due to the relatively long timescale of each "experiment" although this would be less noticeable in a temperature controlled climatic store. The influence of temperature is seen as a diurnal variation in the conductivity, small compared to the measured ageing effects, which we believe could be accounted for in the observed trends over long time periods so that the impact of cyclic temperature variations (such as might be observed in freeze–thaw stability trials) can be separated from longer term, deterioration of stability (which could be days, weeks or months).

More validation of tomographic measurements is required by further conductivity measurements. This will enable a better understanding of the true meaning of reconstructed images using the 'difference imaging' method. In addition, for long term stability, instrument issues such as drift from the reference frame could become pronounced and will need to be assessed to ensure that this is not mistaken as the onset of a stability problem.

Future efforts will explore the use of a finer mesh, say 10,000 elements, to improve resolution in selected regions of the vessel. We also intend to explore the use of base-mounted electrodes, in a similar way to that used previously for pressure filtration [32]. The 3D penetration of the electric field will provide more detailed examination in the region of the base.

References

[1] C.D. Vaughan, in: D. Laba (Ed.), Predicting Stability in Rheologically Modified Systems in Rheological Properties of Cosmetics and Toiletries, Marcel Dekker Inc., 1993.
[2] P.E. Miner, in: D. Laba (Ed.), Emulsion Rheology: Creams and Lotions in Rheological Properties of Cosmetics and Toiletries, Marcel Dekker Inc., 1993.
[3] P.D.T. Huibers, D.O. Shah, A.R. Katritzky, Predicting surfactant cloud point from molecular structure, J. Colloid Interface Sci. 193 (1997) 132–136.
[4] D.J. Mitchell, G.J.T. Tiddy, L. Waring, T. Bostock, M.P. McDonald, Phase-behaviour of polyoxyethylene surfactants with water–mesophase structures and partial miscibility (cloud points), J. Chem. Soc., Faraday Trans. 79 (1983) 975–1000.
[5] D.L. Hoffman, D.R. Brooks, P.I. Dolez, B.J. Love, Design of a *z*-axis translating laser light scattering device for particulate settling measurement in dispersed fluids, Rev. Sci. Instrum. 73 (2002) 2479–2482.
[6] H. Mahgerefteh, D. Kamugasha, Novel on-line sedimentation analyser, J. Colloid Interface Sci. 228 (2000) 410–422.
[7] V.J. Pinfield, M.J.W. Povey, E. Dickinson, Interpretation of ultrasound velocity creaming profiles, Ultrasonics 34 (1996) 695–698.
[8] O.-P. Tossavainen, M. Vauhkonen, V. Kolehmainen, K.Y. Kim, Tracking of moving interfaces in sedimenation processes using electrical impedance tomography, Chem. Eng. Sci. 61 (2006) 7717–7729.
[9] D. Vlaev, M. Wang, T. Dyakowski, R. Mann, B.D. Grieve, Detecting filter-cake pathologies in solid-liquid filtration: semi-tech scale studies using electrical resistance tomography, Chem. Eng. J. 77 (2000) 87–91.
[10] J.A. Gutierrez, T. Dyakowski, M.S. Beck, R.A. Williams, Using electrical impedance tomography for controlling hydrocyclone underflow discharge, Powder Technol. 108 (2000) 180–184.
[11] M.D. Garcia, M. Orea, L. Carbognami, A. Urbana, The effect of paraffinic fractions on crude oil wax crystallization, Pet. Sci. Technol. 19 (2001) 189–196.
[12] W.J. Weber, Physicochemical Process for Water Quality Control, Wiley-Interscience, New York, 1972, p. 111.
[13] F. Ricard, C. Brechtelsbauer, X.Y. Xu, C.J. Lawrence, Monitoring of multiphase pharmaceutical processes using electrical resistance tomography, Chem. Eng. Res. Des. 83 (2005) 794–805.
[14] H.I. Schlaberg, J.H. Bass, M. Wang, J.L. Best, R.A. Williams, J. Peakall, Electrical resistance tomography for suspended sediment measurements in open channel flows using a novel sensor design part, Part. Syst. Charact. 23 (2006) 313–320.
[15] M.M. Rieger, Stability testing of macroemulsions, Cosmet. Toilet. 106 (1991) 59–69.
[16] D.R. Karsa, Industrial Applications of Surfactants, The Royal Society of Chemistry, London, 1986.
[17] C. Wilson, The History of Unilever: A Study in Economic Growth and Social Change, vol. 1, Cassell, London, 1954.
[18] J.R. Stokes, J.H. Telford, Measuring the yield behaviour of structured fluids, J. Non-Newton. Fluid Mech. 124 (2004) 137–146.
[19] M.G. Berni, C.J. Lawrence, D. Machin, A review of the rheology of the lamellar phase in surfactant systems, Adv. J. Colloid Interface Sci. 98 (2002) 217.

[20] J. Nakarapanich, T. Barameesangpet, S. Suksamranchit, A. Sirivat, A. Jamieson, Rheological properties and structures of cationic surfactants and fatty alcohol emulsions: effect of surfactant chain length and concentration, Colloid Polym. Sci. 279 (2001) 671.
[21] J. Szymanski, A. Wilk, R. Holyst, G. Roberts, A. Kowalski, K. Sinclair, Micro & macro shear viscosity in dispersed lamellar phases, J. Non-Newton. Fluid Mech. 148 (2008) 134.
[22] E. van der Linden, W.T. Hogervorst, H.N.W. Lekkerkerker, Relation between the size of lamellar droplets in onion phases and their effective surface tension, Langmuir 12 (1996) 3127–3130.
[23] G. Eccleston, Structure and rheology of pharmaceutical and cosmetic creams–cetrimide creams—influence of alcohol chain-length and homolog composition, J. Colloid Interface Sci. 57 (1976) 66–74.
[24] A. Goldszal, A. Jamieson, J.A. Mann, J. Polak, C. Rosenblatt, Rheology, optical microscopy, and electron microscopy of cationic surfactant gels, J. Colloid Interface Sci. 180 (1996) 261–268.
[25] M. Yoon, Y. Chung, K. Han, A study of gel structure in the nonionic surfactant/cetostearyl alcohol/water ternary systems by differential scanning calorimeter, J. Disper. Sci. Technol. 20 (1999) 1695–1713.
[26] O. Diat, D. Roux, F. Nallet, Effect of shear on a lyotropic lamellar phase, J. Phys. II Fr. 3 (1993) 1427–1452.
[27] P. Partal, A. Kowalski, D. Machin, N. Kiratziz, M. Berni, C. Lawrence, Rheology and microstructural transitions in the lamellar phase of a cationic surfactant, Langmuir 17 (2001) 1331.
[28] G. Akay, G.N. Irving, A.J. Kowalski, D. Machin, Patent WO9620270 A1.
[29] Y. Yamagata, M. Senna, Effects of temperature on the development of the internal structure of the cetyltrimethylammonium chloride/cetyl alcohol/water system, Langmuir 15 (1999) 7461–7463.
[30] T.A. York, S. Murphy, A. Burnett-Thompson, B.D. Grieve, An accessible electrical impedance imaging system, in: 4th World Congress on Industrial Process Tomography, Aizu, Japan, September 5–8, 2005, pp. 100–105.
[31] T.A. York, J.L. Davidson, L. Mazurkiewich, R. Mann, B.D. Grieve, Towards process tomography for monitoring pressure filtration, IEEE Sens. J. 5 (2) (2005) 139–152.
[32] J.L. Davidson, L.S. Ruffino, D.R. Stephenson, R. Mann, B.D. Grieve, T.A. York, Three-dimensional electrical impedance tomography applied to a metal-walled filtration test platform, Meas. Sci. Technol. 15 (2004) 2263–2274.
[33] N. Polydorides, W.R. Lionheart, A MatLab based toolkit for three-dimensional electrical impedance tomography: a contribution to the EIDORS project, Meas. Sci. Technol. 13 (2002) 1871–1883.
[34] D.R. Stephenson, J.L. Davidson, W.R.B. Lionheart, B.D. Grieve, T.A. York, Comparison of 3-D image reconstruction techniques using real electrical impedance measurement data, in: 4th World Congress on Industrial Process Tomography, Aizu, Japan, September 5–8, 2005, pp. 643–650.
[35] D.R. Stephenson, R. Mann, T.A. York, The sensitivity of reconstructed images and process engineering metrics to key choices in practical electrical impedance tomography, Meas. Sci. Technol. 19 (September (9)) (2008), paper 094013. http://www.iop.org/EJ/toc/0957-0233/19/9.
[36] P.L. Goggin, R. He, D.Q.M. Craig, D.P. Gregory, An investigation into the supramolecular structure of ternary gel systems using oscillatory rheometry, microscopy and low frequency dielectric spectroscopy, J. Pharm. Sci. 88 (1999) 661–669.
[37] P.L. Goggin, R. He, D.Q.M. Craig, D.P. Gregory, An investigation into the use of low-frequency dielectric spectroscopy as a means of characterising the structure of creams based on aqueous cream BP, J. Pharm. Sci. 87 (1998) 559–564.
[38] R. He, D.Q.M. Craig, Characterisation of the effects of drug addition on the structure of glycerol monoolein/water gel systems using low frequency dielectric spectroscopy, J. Pharm. Sci. 88 (1999) 635–639.